*Progress In Electromagnetics Research B, Vol. 21, 151–170, 2010*

# EFFICIENT ELECTRICALLY SMALL OBLATE SPHEROIDAL AND SPHERICAL ANTENNAS IN SHELLS WITH NEGATIVE PERMITTIVITY

**O. B. Vorobyev**

Stavropol Institute of Radiocommunications
Russia

**Abstract**—Electrically small oblate spheroidal and spherical antennas in confocal shells with negative permittivity represent perspective antenna design to combine moderately small size, wide bandwidth, high efficiency and power of radiation. However, optimization of the antennas performance parameters imposes contradictory restrictions on permittivity of the shells, electrical size of the antennas, shape of the antennas and shells. Simulation results based on method of eigen-functions have shown that the antennas can be tuned on resonance for small magnitudes of negative permittivity of the shells and antiresonance for higher magnitudes. Optimal combination of power and efficiency of radiation of the antenna and the quality factor is obtained in an intermediate range of negative permittivity by combining merits of resonance and antiresonance of the antenna.

Antiresonant range of the oblate spheroidal antenna emerges for lower permittivity magnitudes as compared with the spherical antenna. As a result, the optimal size of the shell of oblate spheroidal antenna is comparatively small. However, more gradual emerging of antiresonant properties of the spherical antenna makes spherical design more suitable for higher level of inherent absorption of the shell medium with negative permittivity.

## 1. INTRODUCTION

Optimization of electrically small dipole antennas in shells with negative permittivity have been given considerable attention in recent years. It was found that the antenna shells of different shapes with one or several shell layers can be used to tune the antennas on resonance in order to increase their power of radiation [1–11].

Corresponding author: O. B. Vorobyev (olegbvorobyev@gmail.com).

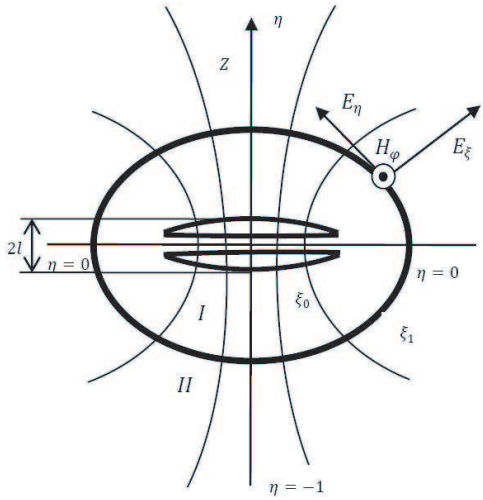


**Figure 1.** Oblate spheroidal coordinate system $\xi, \eta, \varphi$ (cross-section by plane $\varphi = const, const + \pi$). Coordinate surfaces: confocal oblate ellipsoids of rotation (in relation to the axis $Z$), one-sheet hyperboloids, and semi-planes accordingly; $\xi = \xi_0$ — surface of the antenna divided by a narrow feed gap, $2l$ — height of the antenna, $\xi = \xi_1$ — an outer boundary of antenna shell defined by condition of maximum power of radiation.

A series LC circuits have been used to model the antennas tuned on resonance by the shells. According to the model, inherent negative reactance of an electrically small dipole antenna in free space can be compensated by positive reactance of the antenna shell [1, 5, 8]. Input voltage of the antenna tuned on resonance is applied to the antenna resistance. As a result, input current of the antenna is maximal. Power of radiation of the antenna and electrical polarization of some regions of shell medium around the upper and lower antenna ends (Fig. 1) are maximal too. Axial symmetry of the antenna assumes a fan of directions of polarization and displacement current in the shell around the antenna. Therefore, dipole moment of the shell and power of its radiation is small.

More uniform polarization of shell medium can be created by an external quasi-static electric field [2, 7] even without an antenna inside the shell with negative permittivity. Because of a non-zero dipole moment of the shell, the shell becomes a source of scattered radiation. A similar electric field can be created by the antenna inside of the shell [2, 7]. Nevertheless, resonant polarization of shell medium of the antenna tuned on resonance or antiresonance and resonant

polarization of a dielectric resonator with negative permittivity in an external uniform quasi-static electric field are different condition in contradiction with [2, 10, 11]. Connection of all kinds of resonant polarization with the parameters of antennas, such as the quality factor, radiation efficiency, and others, needs additional clarification.

Parameters of antennas, such as impedance, return loss, relative gain, are commonly presented as functions of frequency, whereas it is obvious that resonant and antiresonant values of the parameters are the most important. Frequency dependencies of the parameters of the antenna in the shell additionally depend on permittivity (or plasma frequency), electrical size, shape of the shell and antenna. It is reasonable to simplify the study approach by choosing resonant conditions as base features of the antenna to temporarily neglect dependence from frequency. Comparing resonant conditions, it is possible to select the optimal condition being characterized by permittivity of the shell and its electrical size. Using the found optimal condition, frequency dependence of the antenna parameters can be easily calculated with an appropriate dispersion of permittivity of the shell.

It is well known that a quasi-static resonant polarization of a sphere with negative permittivity in an external uniform quasi-static electric field is solely defined by permittivity of the sphere and has narrow width of resonance. In case of non-infinitesimal size of the sphere, the width of the resonant curve of polarization is an increasing function of electrical size of the sphere [2]. Additionally, scattering efficiency is an increasing function of electrical size of the sphere [2]. Assuming analogy, one can expect that small electrical size of the shell with negative permittivity may prevent combining of the antenna performance parameters with optimal values, which need different conditions of the shell polarization. Upper electrical size of an electrically small antenna is limited by condition $ka \leq 0.5$, where $a$ — radius of a minimal imaginary sphere enclosing the antenna shell, $k$ — the wave number. Therefore, the electrical size of the antenna in the shell have to be chosen equal to the maximal size of electrically small antenna, $ka \approx 0.5$.

Simulation of the antenna parameters was conducted for the oblate spheroidal and spherical antennas. Although prolate antennas in the shells of different shapes represent the most discussed antenna design, the oblate shape of antenna has evident advantages, such as low antenna reactance and a more uniform electric field in the antenna shell. Using a half of an oblate spheroid above a ground plane, it is possible to replicate parameters of the whole oblate spheroidal antenna [12]. In such case, a half of the oblate spheroidal antenna

above a ground plane has similarity with an electrically small patch antenna. Therefore, the electrically small oblate spheroidal antenna with low value of length-to-diameter ratio (sphericity) can be also used as approximation of a planar antenna design.

## 2. ELECTROMAGNETIC FIELD OF THE OBLATE SPHEROIDAL ANTENNA IN THE CONFOCAL SHELL WITH NEGATIVE PERMITTIVITY

### 2.1. Field Equations and Boundary Conditions

Numerical simulation of the antennas in confocal shells has been done by solving of a boundary-value problem in oblate spheroidal coordinate system.

Structure of the oblate spheroidal antenna in the shell is shown in Fig. 1. The antenna consists from two oblate semi-ellipses with the axis of rotation $Z$. Semi-ellipses are separated from each other by the narrow gap with sides coordinates $-\eta',\ \eta', (\eta' = 0.05)$. The antenna is covered by a confocal layer of substance (metamaterial, plasma) with complex permittivity. The height of the antenna is $2l$.

As a consequence of the axial symmetry, $\frac{\partial}{\partial\varphi} = 0$. Maxwell's system of field equations with time dependency $e^{i\omega t}$ is [7]

$$\begin{aligned} &\frac{1}{h_\eta h_\varphi}\frac{\partial}{\partial\eta}\left(h_\varphi H_\varphi\right) = i\omega\varepsilon\varepsilon_0 E_\xi, \quad -\frac{1}{h_\xi h_\varphi}\frac{\partial}{\partial\xi}\left(h_\varphi H_\varphi\right) = i\omega\varepsilon\varepsilon_0 E_\eta, \\ &\frac{1}{h_\xi h_\eta}\left[\frac{\partial}{\partial\xi}\left(h_\eta E_\eta\right) - \frac{\partial}{\partial\eta}\left(h_\xi E_\xi\right)\right] = -i\omega\mu\mu_0 H_\varphi. \end{aligned} \tag{1}$$

where $(\xi, \eta, \varphi)$ oblate spheroidal coordinates, $0 \le \xi < \infty,\ -1 \le \eta \le 1,\ \ 0 \le \varphi < 2\pi$. Metric coefficients $h_\xi,\ h_\eta, h_\varphi$ are

$$\begin{aligned} h_\xi &= \frac{d}{2}\left(\frac{\xi^2+\eta^2}{\xi^2+1}\right)^{1/2}, \quad h_\eta = \frac{d}{2}\left(\frac{\xi^2+\eta^2}{1-\eta^2}\right)^{1/2}, \\ h_\varphi &= \frac{d}{2}\left[\left(\xi^2+1\right)\left(1-\eta^2\right)\right]^{1/2}, \end{aligned} \tag{2}$$

where $\varepsilon_0$, $\mu_0$ — electric and magnetic constants, $\varepsilon = \varepsilon(\omega) = \varepsilon'(\omega) - i\varepsilon''(\omega)$ — complex relative permittivity, $\mu$ — relative permeability, $d$ — focal distance.

Expressing $E_\xi$ and $E_\eta$ by the first two equations (1) to use in the third one, one finds equation for $H_\varphi$

$$\begin{aligned} &\sqrt{\xi^2+1}\frac{\partial^2}{\partial\xi^2}\left(\sqrt{\xi^2+1}H_\varphi\right) + \sqrt{1-\eta^2}\frac{\partial^2}{\partial\eta^2}\left(\sqrt{1-\eta^2}H_\varphi\right) \\ &= -c^2\left(\xi^2+\eta^2\right)H_\varphi, \end{aligned} \tag{3}$$

where $c = \frac{k'd}{2}$, $k' = \omega\sqrt{\mu\mu_0\varepsilon\varepsilon_0}$ — the wave number.

The Equation (3) allows separation of variables [15]

$$H_\varphi(\xi,\eta) = P(\xi)\,Q(\eta). \tag{4}$$

Substituting (4) into (3), one finds two Sturm-Liouville's equations for the oblate angular and radial spheroidal eigen-functions [13–15]

$$\begin{aligned} &\frac{d}{d\eta}\left[\left(1-\eta^2\right)\frac{dQ}{d\eta}\right] + \left(c^2\eta^2 + \lambda - \frac{1}{1-\eta^2}\right)Q = 0, \\ &\frac{d}{d\xi}\left[\left(\xi^2+1\right)\frac{dP}{d\xi}\right] + \left(c^2\xi^2 - \lambda + \frac{1}{\xi^2+1}\right)P = 0, \end{aligned} \tag{5}$$

where $\lambda$ — constant of separation of variables linking radial and angular functions $P(\xi)$, $Q(\eta)$. A non-trivial solution of equations (5) exists for discrete values $\lambda = \lambda_{1n}(c)$, which are numbered in increasing order and called the eigen-values. $Q(\eta)$ is being represented by a series of oblate angular spheroidal functions of the first kind, while $P(\xi)$ in general case is being represented by a series of oblate radial spheroidal functions of the third and fourth kind, which represent electromagnetic waves coming to the source and outgoing to infinity.

To build general solution of the problem, expressions for the field vectors were written for two areas: the antenna shell I (Fig. 1), and free space around antenna II. Vectorial components of electromagnetic field for the antenna shell are

$$\begin{aligned} H_\varphi^I &= \sum_{n=1,3,\ldots}^{\infty} S_{1n}^{(1)}(-ic\alpha,\ \eta)\times\left[a_n R_{1n}^{(3)}(-ic\alpha, i\xi) + b_n R_{1n}^{(4)}(-ic\alpha, i\xi)\right], \\ E_\xi^I &= \frac{2}{i\omega d\varepsilon_0\ \varepsilon(\xi^2+\eta^2)^{0.5}} \\ &\quad\times\sum_{n=1,3,\ldots}^{\infty}\left[a_n R_{1n}^{(3)}(-ic\alpha, i\xi) + b_n R_{1n}^{(4)}(-ic\alpha, i\xi)\right] \\ &\quad\times\frac{\partial}{\partial\eta}\left(\left(\sqrt{1-\eta^2}\right)S_{1n}^{(1)}(-ic\alpha,\eta)\right), \\ E_\eta^I &= \frac{2}{\omega d\varepsilon_0\ \varepsilon(\xi^2+\eta^2)^{0.5}} \\ &\quad\times\sum_{n=1,3,\ldots}^{\infty} S_{1n}^{(1)}(-ic\alpha,\eta)\left[a_n\frac{\partial}{\partial\xi}\left(\sqrt{\xi^2+1}R_{1n}^{(3)}(-ic\alpha,\ i\xi)\right)\right. \\ &\quad\left. + b_n\frac{\partial}{\partial\xi}\left(\sqrt{\xi^2+1}R_{1n}^{(4)}(-ic\alpha, i\xi)\right)\right], \end{aligned} \tag{6}$$

where $S_{1n}^{(1)}(-ic\alpha,\ \eta)$ — Flammer's angular spheroidal function of the first kind, $R_{1n}^{(3)}(-ic\alpha,\ i\xi)$, $R_{1n}^{(4)}(-ic\alpha,\ i\xi)$ — Flammer's radial spheroidal function of the 3 and 4 kinds [14–17], $c = \frac{kd}{2}$, $k = \omega\sqrt{\mu_0\varepsilon_0}$ — the wave number in free space, $\alpha = \sqrt{\varepsilon}$, $\varepsilon$ — relative permittivity of the antenna shell, $a_n$, $b_n$ — coefficients defined by boundary conditions.

Vectorial components of electromagnetic field of the oblate antenna in free space around the shell are

$$\begin{aligned}
H_{\varphi}^{II} &= \sum_{n=1,3,\ldots}^{\infty} S_{1n}^{(1)}(-ic,\ \eta)\, g_n R_{1n}^{(4)}(-ic,\ i\xi)\ , \\
E_{\xi}^{II} &= \frac{2}{i\omega d\varepsilon_0(\xi^2+\eta^2)^{0.5}} \\
&\quad \times \sum_{n=1,3,\ldots}^{\infty} g_n R_{1n}^{(4)}(-ic,\ i\xi)\, \frac{\partial}{\partial\eta}\left(\sqrt{1-\eta^2}\, S_{1n}^{(1)}(-ic,\ \eta)\right), \\
E_{\eta}^{II} &= \frac{2}{\omega d\varepsilon_0(\xi^2+\eta^2)^{0.5}} \\
&\quad \times \sum_{n=1,3,\ldots}^{\infty} S_{1n}^{(1)}(-ic,\ \eta)\, g_n \frac{\partial}{\partial\xi}\left(\sqrt{\xi^2+1}\, R_{1n}^{(4)}(-ic,\ i\xi)\right), \quad (7)
\end{aligned}$$

$g_n$ — coefficient defined by boundary conditions.

Boundary conditions have been formulated so that tangential component of electric field on the antenna surface, $\xi = \xi_0$ in Fig. 1, was zero [7]

$$E_{\eta}^{I}(\xi_0) + E_{\eta ext}^{I}(\xi_0) = 0, \quad (8)$$

where an external field $E_{\eta ext}^{I}(\xi_0)$ between semi-spheroids is defined by feed voltage $U$ of the antenna. Tangential components of electromagnetic field on the boundary of the antenna shell with free space ($\xi = \xi_1$) are continuous $E_{\eta}^{I} = E_{\eta}^{II}$, ($\xi = \xi_1$), $H_{\varphi}^{I} = H_{\varphi}^{II}$, ($\xi = \xi_1$).

### 2.2. Formulas for Calculation of Antenna Parameters

The antennas performance parameters have been calculated on base of the simulated electromagnetic field.

Current of conductivity of the oblate spheroidal antenna is

$$I_{\eta}(\xi_0,\eta) = \int_0^{2\pi} j_{\eta}(\xi_0,\eta)\, h_{\varphi} d\varphi = H_{\varphi}^{I}(\xi_0,\eta)\, \pi d\sqrt{\left(\xi_0^2+1\right)(1-\eta^2)}, \quad (9)$$

where $j_\eta(\xi_0, \eta)$ — density of current on the antenna surface. Therefore, input current is

$$I_0 = I_0(\xi_0) = H_\varphi^I(\xi_0, \eta')\,\pi d\sqrt{\left(\xi_0^2+1\right)\left(1-[\eta']^2\right)}, \tag{10}$$

where $\eta = \pm\eta'$ coordinates of the input points of the antennas.

Shell current ($\eta = \pm\eta'$) is

$$I_0(\xi_1) = H_\varphi^I(\xi_1, \eta')\,\pi d\sqrt{\left(\xi_1^2+1\right)\left(1-[\eta']^2\right)} - I_0. \tag{11}$$

The input impedance of the antenna is

$$Z = U/I_0. \tag{12}$$

Total radiated power of the antenna [7] calculated in far field is

$$P_{\mathcal{R}} = \frac{1}{2}\mathrm{Re}\int\limits_{\xi\to\infty} E_\eta^{II} H_\varphi^{II*} h_\eta h_\varphi d\eta d\varphi = \frac{\pi}{k\omega_0\varepsilon_0}\sum_{n=1,3,\ldots}^{\infty} N_{1n}(c)|g_n|^2, \tag{13}$$

where the surface integral is taken with $\xi \to \infty$, the superscript $H_\varphi^{II*}$ denotes the complex conjugate, sum is taken for odd $n$ to calculate radiation of the first modes, including $\mathrm{TM}_{1n}$. Coefficients $N_{1n}(c)$ are determined by the orthogonality condition

$$N_{1n}(c)\,\delta_{nm} = \int_{-1}^{1} S_{1n}^{(1)}(-ic,\ \eta) S_{1m}^{(1)}(-ic,\ \eta)\,d\eta. \tag{14}$$

Radiation resistance of the antenna is

$$R_{\mathcal{R}} = 2P_{\mathcal{R}}/|I_0|^2. \tag{15}$$

The antenna radiation efficiency is

$$\eta_r = P_{\mathcal{R}}/P_{\mathrm{A}} = 2P_{\mathcal{R}}/U\mathrm{Re}(I_0), \tag{16}$$

where $P_A$ — power accepted by an antenna. Power accepted by an antenna [18] is

$$P_{\mathrm{A}} = \frac{1}{2}|I_0|^2 R = \frac{1}{2}|U|^2 G, \tag{17}$$

where $R$ — antenna resistance, $G$ — antenna conductance, $G = \mathrm{Re}[1/Z]$ [18] (resistance and reactance of the feed line of the antenna and its voltage supply are considered small as compared with impedance of the antenna).

The quality factor of an antenna tuned at frequency $\omega_0$ is [18]

$$Q(\omega_0) = \frac{\omega\,|W(\omega_0)|}{P_A(\omega_0)}, \tag{18}$$

where $W(\omega_0)$ — time-averaged energy of non-propagating electromagnetic field.

The approximate quality factor of an antenna tuned at frequency $\omega_0$ is [18]

$$Q_Z(\omega_0) \approx \frac{\omega_0}{2R_0(\omega_0)} \sqrt{[R'(\omega_0)]^2 + \left[X'(\omega_0) + \left|\frac{X(\omega_0)}{\omega_0}\right|\right]^2}, \qquad (19)$$

where $R(\omega)$ and $X(\omega_0)$ are resistance and reactance of the tuned or even untuned antenna, $\omega_0$ — frequency of the antenna in resonance or antiresonance range, primes stand for frequency derivatives.

The lower bound on the antenna quality factor is [19, 20]

$$Q_{lb} = \eta_r \left(\frac{1}{k^3 a^3} + \frac{1}{ka}\right), \qquad (20)$$

where $a$ — radius of a minimal imaginary sphere enclosing the antenna shell, $k$ — the wave number of radiation. The lower bound on the quality factor is equal to the quality factor of the spherical antenna with electrical size $ka$ for $\mathrm{TM}_{01}$ spherical mode (in the case of absence of stored energy inside of the antenna).

Calculations of the quality factor with (18) are based on rather complex numerical evaluations of $W(\omega_0)$ [22]. Convenient form of the exact quality factor (18) for an antenna is [18]

$$Q(\omega_0) = \frac{\omega_0}{2R_0(\omega_0)} \left| X_0'(\omega_0) - \frac{4}{|I_0|^2} \left[W_{\mathcal{L}}(\omega_0) + W_{\mathcal{R}}(\omega_0)\right] \right|, \qquad (21)$$

where $W_{\mathcal{L}}(\omega_0)$ — time-averaged energy of losses of electromagnetic field (for lossless antenna material $W_{\mathcal{L}}(\omega_0) = 0$), $W_{\mathcal{R}}(\omega_0)$ — energy of antenna radiation. Derivation of an expression for energy of antenna radiation in oblate spheroidal coordinate system is given in the appendix.

## 3. RESULTS OF CALCULATIONS

### 3.1. Parameters of the Antennas in Free Space

A computer program calculating parameters of the spherical and oblate spheroidal antennas in free space and in the shells with negative real part of permittivity was created on base of the computer algebra system Wolfram Mathematica.

Parameters of the antennas given by surfaces $\xi_0 = 0.1005,\ 10.05$ were studied. Height of the oblate spheroidal antenna in Fig. 1 with the spheroidal surface $\xi = \xi_0$ is

$$2l = d\xi_0. \qquad (22)$$

The antenna diameter in the plane perpendicular to the axis of symmetry $Z$ is

$$2R(\xi_0, \eta) = d\left[\left({\xi_0}^2 + 1\right)\left(1 - \eta^2\right)\right]^{1/2}. \tag{23}$$

Electrical sizes $kl$, $kR$ of the oblate spheroidal and spherical antennas are shown in Table 1.

**Table 1.** Parameters of oblate spheroidal ($TM_{11}$) and spherical antennas ($TM_{01}$) in free space.

| | | | |
|---|---|---|---|
| $\xi_0$ | Coordinate of the antenna surface | 0.1005 | 10.05 |
| $kl$ | Electrical size (in direction of the height) | 0.019 | 0.19 |
| $kR$ | Electrical size (in direction of the radius) | 0.19 | 0.19 |
| $S$ | Sphericity of the antenna | 0.1 | 1 |
| $P$ | Power of radiation ($W$), ($U = 1\,\mathrm{V}$) | $1.4 \times 10^{-6}$ | $8.7 \times 10^{-6}$ |
| $R_\Sigma$ | Radiation resistance ($\Omega$) | 0.61 | 2.8 |
| $X$ | Reactance ($\Omega$) | $-i480$ | $-i403$ |
| $Q_{lb}$ | The lower bound on the quality factor | 149 | 149 |
| $Q/Q_{lb}$ | The normed quality factor | 5.33 | 1 |

Shape of the spheroidal antenna together with electrical size is one from the most important parameters of antenna. There are several terms for the parameter of shape with close meanings, including length-to-diameter ratio for cylindrical antennas [21], and ellipticity for spheroidal antennas [22]. Circumscribed spheres of spheroidal and cylindrical antennas with the same length-to-diameter ratio have different diameters. Because of reference to the spherical antenna in the definition of the lower bound on the quality factor (20), it seems more intensional to describe the antenna by its sphericity. Similar to ellipticity and length-to-diameter ratio, sphericity is equal to ratio of the height of the oblate spheroidal antenna to its diameter at the middle part. Sphericity of the antenna with the surface $\xi = \xi_0$, is

$$S = \frac{\xi_0}{\left({\xi_0}^2 + 1\right)^{1/2}}. \tag{24}$$

In general case, sphericity of the antennas can be defined as ratio of length-to-diameter where the bigger size is the diameter of the circumscribed sphere. Definition (24) for a spheroidal antenna gives the same value of sphericity as the more general definition.

The quality factor of an antenna is function of electrical size of the reference spherical antenna $Q_{lb}$ (20) and degree of using of the spherical volume by the antenna [21, 23, 24]. For comparison of the antennas

with different shape, size, and regime of radiation, it is convenient to present the quality factors of the antennas as ratio of the quality factor to the quality factor of the reference spherical antenna (20) similar to the quality factors of cylindrical antennas in [21]. As a result, the antenna is characterized by the normed quality factor $Q/Q_{lb}$, which represents degree of approaching of the quality factor to the lower bound on the quality factor in relative units.

The antenna parameters in Table 1 were simulated for feed voltage with amplitude $U = 1\,\mathrm{V}$ and circular frequency $\omega_0 = 6 \times 10^9$ rad/s. The spherical antenna in vacuum provides higher power of radiation and less the normed quality factor than the oblate spheroidal antenna as a result of lower capacitance reactance and much higher radiation resistance of the spherical antenna.

### 3.2. Parameters of the Antennas in the Shells with Negative Permittivity

Results of calculations of maximum power of radiation of the antennas in the shells with negative permittivity as functions of magnitude of the real part of relative negative permittivity are presented in Fig. 2. Simulated dependencies correspond to the size and shape of the antennas in Table 1. Size of the shell in Fig. 2 for a certain permittivity is defined by provision of maximal power of radiation of the antenna.

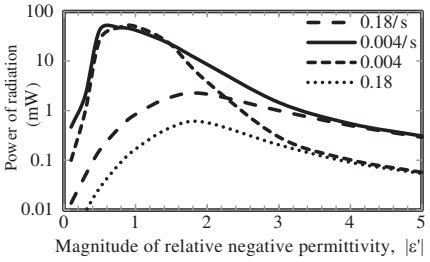


**Figure 2.** Maximum power of radiation (in logarithmic scale) of the oblate spheroidal ($d = 0.019\,\mathrm{m}$) and the spherical antennas ($d = 0.0019\,\mathrm{m}$) in the shells with $\varepsilon'' = 0.004, 0.18$ is shown as functions of magnitude of the real part of relative negative permittivity $|\varepsilon|'$ (feed voltage $U = 1\,\mathrm{V}$).

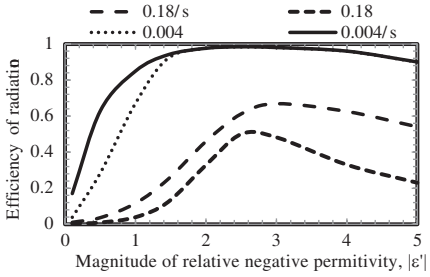


**Figure 3.** Efficiency of radiation of the oblate spheroidal and the spherical antennas in the shells with $\varepsilon'' = 0.004, 0.18$ as functions of magnitude of the real part of relative negative permittivity $|\varepsilon'|$.

Curves in the legend with index s correspond to the spherical antenna. Curves in the legend in Fig. 2 without letter index correspond to the oblate spheroidal antenna. Simulated results for antennas radiation were calculated for two levels of losses $\varepsilon'' = 0.004,\ \ 0.18$ for both antennas. Values of $\varepsilon''$ are used to mark the curves in the legend. Calculated power of radiation is presented in milliwatts (feed voltage 1V) as function of magnitude of the real part of relative negative permittivity of the shell, which is called hereinafter as permittivity magnitude.

Power of radiation of the spherical and spheroidal antennas in the shells in Fig. 2 is much higher as compared with antennas in free space in Table1. Common feature of the dependencies is comparatively low power of radiation for magnitudes of negative permittivity close to zero. Powers of radiation of the antennas reach maximal values with relatively low magnitudes of permittivity of the shells, especially with the lower level of losses. Powers of the antennas radiation are decreasing functions of permittivity magnitude for $|\varepsilon'| \geq 2$ in case of the lower and higher losses in the shells.

An advantage of the spherical antenna is higher power of radiation as compared with the oblate spheroidal antenna for almost all conditions in Fig. 2. However, maximal powers of radiation of both antennas are commensurate for smaller level of losses.

Comparison of the antennas radiation for the two levels of losses in the antennas shells shows that degree of diminishing of maximal values of the antennas radiation correlates with degree of increasing of $\varepsilon''$. Power of radiation of both antennas becomes almost independent from level of losses for $|\varepsilon'| \geq 3$ that implies cardinal changes in radiation mechanism of the antennas.

Radiation efficiency of the antennas is presented in Fig. 4. Efficiencies of both antennas are low while real part of negative permittivity is close to zero. It explains low power of radiation for small magnitudes of permittivity in Fig. 2. Radiation efficiency reaches maximal values with increase of permittivity magnitude. Maximal values of efficiency correspond to higher permittivity magnitude as compared with power of radiation in Fig. 2. Advantage of the spherical antenna is a better overlapping of ranges of high efficiency and power of radiation.

Resistance of radiation of the spherical and oblate spheroidal antennas as functions of permittivity magnitude is presented in Fig. 4. All curves represent a resonance-like pattern. Higher radiation resistance corresponds to lower level of losses in the shells.

Permittivity range of high efficiency of radiation in Fig. 3 corresponds to the range of permittivity of maximal resistance of

radiation in Fig. 4. Increase of radiation resistance and efficiency corresponds to decrease of power of radiation in Fig. 2. Wider curve of radiation resistance of the spherical antenna as compared with the curve of the oblate spheroidal antenna correlates with the lower slopes of dependencies of efficiency and power of radiation for the spherical antenna.

Dependences of reactance of the antennas from negative permittivity magnitude are showed in Fig. 5. All dependencies correspond to maximum power of radiation for the given size and shape of the antennas in Table I. The antennas with lower level of losses are tuned on zero reactance over the range of negative permittivity $|\varepsilon'| \approx 0, \ldots, 2$. Reactance of both antennas, tuned on maximum power of radiation in the range of small magnitudes of negative permittivity, is eliminated by the shells with the higher level of losses only partly ($|\varepsilon'| \leq 0.5$ , $\varepsilon'' = 0.18$).

Zero reactance and maximal power of radiation of an antenna are requisite ingredients of resonance. Therefore, according with Fig. 5, resonance range of the antennas with the lower level of losses corresponds to permittivity range $|\varepsilon'| \approx 0, \ldots, 1.5$. Because of non-zero reactance for small magnitudes of negative permittivity, regime of maximum power of the antennas with the higher level losses in resonance range is not resonance regime. Higher power of radiation in the latter case corresponds to partly tuned antennas because of low radiation efficiency for small magnitudes of negative permittivity. Antennas with the higher level of losses can be tuned on resonance in resonance range with lower power of radiation and efficiency.

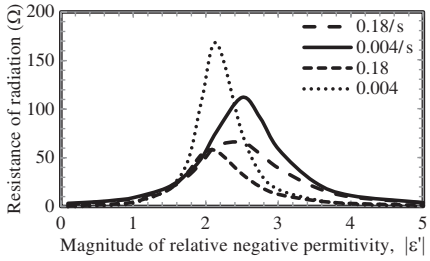


**Figure 4.** Resistance of radiation of the oblate spheroidal and the spherical antennas in the shells with $\varepsilon'' = 0.004, 0.18$ as functions of magnitude of the real part of relative negative permittivity $|\varepsilon'|$.

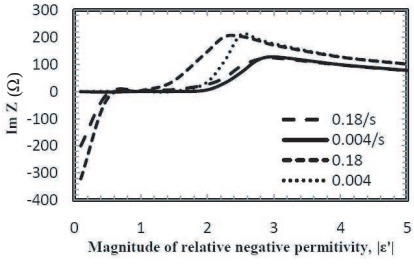


**Figure 5.** Reactance of the oblate spheroidal and the spherical antennas in the shells with $\varepsilon'' = 0.004, 0.18$ as functions of magnitude of the real part of relative negative permittivity $|\varepsilon'|$.

Reactance of the antennas is inductive for $|\varepsilon'| \geq 1.5$ while efficiencies of radiation are close to their maximums (Fig. 3, Fig. 5). Decreasing of antennas power of radiation, when $|\varepsilon'|$ is rising over the range $|\varepsilon'| \approx 2, \ldots, 3$ (Fig. 2), is complemented with rising of resistance of radiation. Those conditions of the electrically small antennas in the shells with negative permittivity being conditions of maximum power of radiation are not resonance conditions. However, feed lines of electrically small antennas are also electrically small. As a result, problem of reflection at an interface of the antenna and the feed line does not exist for an electrically small antenna even with non-zero reactance. Therefore, the latter conditions should be included in the examination.

Increase of radiation resistance of the spheroidal and spherical antennas with increase of negative permittivity magnitude (Fig. 4) implies emerging of resonance of currents in the antenna circuit. Resonance of currents in the shell is directly detected by comparison of the shell current with the antenna current. Dependencies of magnitude of the ratio of $\eta$ — component of displacement current of the shell to the input antenna current, $C = |I_0(\xi_1)/I_0|$, $\eta = \eta'$, as functions of permittivity magnitude are presented in Fig. 6.

Parameter $C$ is small over range of permittivity $|\varepsilon'| < 1.5$. Therefore, $\eta$ — component of displacement current in the shell is comparatively small in resonance range, while displacement current of

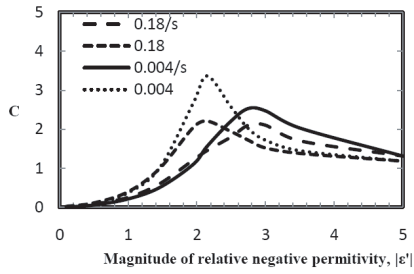


**Figure 6.** Ratio of $\eta$ — component of displacement current in the shell to input antenna current $C = |I_0(\xi_1)/I_0|$ taken at $\eta = \eta'$ as functions of magnitude of the real part of relative negative permittivity $|\varepsilon'|$ for the oblate spheroidal and spherical antennas in the shells with $\varepsilon'' = 0.004, 0.18$.

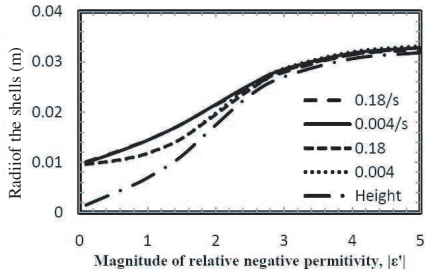


**Figure 7.** Radii of the shells of the spherical antenna (/s) and semiaxes of the oblate spheroidal antenna (height) with $\varepsilon'' = 0.004, 0.18$ are presented as functions of magnitude of the real part of relative negative permittivity $|\varepsilon'|$.

the antenna is concentrated in free space around the shell. Parameter $C$ is higher than the unity over permittivity range $|\varepsilon'| > 2$. Therefore, the shell and free space around the shell (Fig. 1) make up together a parallel resonance loop, which is being tuned on currents resonance with permittivity and size of the shell.

Parameter $C$ in Fig. 6 corresponds to regime of maximum power of radiation, while maximum values of the $C$ match non-zero reactance in Fig. 5. Therefore, currents resonance in the parallel resonance loop produces the condition, which is not resonance or antiresonance of the antenna. This condition has the feature of resonance condition, maximal power of radiation. The other feature of resonance in resonance range, zero reactance cannot be kept in antiresonance range for any level of losses. Zero-reactance in antiresonant range is the feature of antiresonance, which is not compatible with maximal power of radiation. Condition of the antenna with maximum power of radiation in antiresonance range may be called as quasi-resonance. It worth to notice that notion of resonance in antiresonant range is contradictory because zero reactance corresponds both resonant and antiresonant conditions. Therefore, above mentioned condition of resonant scattering of an external quasi-static electric field by a negative permittivity sphere is a quasi-resonance condition with maximum power of radiation of the sphere's medium.

The antennas in the shells with negative permittivity have resonant and antiresonant properties, which depend on shape and electrical size of the antenna, permittivity of the antenna shell. For the given in Table 1 electrical size of the antennas, regime of maximum power defines size of the shells as functions of permittivity. Radius of the shell of the spherical and semiaxes of the oblate spheroidal antennas as functions of permittivity magnitude are presented in Fig. 7. Parameters of the confocal shells, defined by the surface $\xi = \xi_1$ in Fig. 1, are calculated with (22), (23), (24). Sizes of the shells in Fig. 7 are increasing functions of permittivity magnitude for both antennas. Sizes of shells in Fig. 7 extrapolated to $\varepsilon' = 0$ determine sizes of the antennas.

Radii of the shells are shown for two levels of losses. However, sizes of the shells with different levels of losses are so close that difference in the radii can be hardly noticed in Fig. 7. The spheroidal antenna in Fig. 7 is characterized by two dimensions: one of them is the height (23), and the other is the radius (the curve marked in Fig. 7 with values of $\varepsilon''$). The height of the shell of the spheroidal antenna is a comparatively fast increasing function of permittivity magnitude over the range $|\varepsilon'| = 0.1, \ldots, 2$. The height of the shell of the spheroidal antenna becomes almost equal to the shell radius of the spherical

antenna in the range of permittivity $|\varepsilon'| = 2.5, \ldots, 3$. As a result, the size and shape of the shell of the spheroidal antenna becomes almost identical to the size and shape of the shell of the spherical antenna in antiresonance range in Fig. 7.

An advantage of the oblate spheroidal antenna is a comparatively small height of the shell over range of permittivity magnitude $|\varepsilon'| = 1, \ldots, 2$. Power and efficiency of radiation of the oblate spheroidal antenna have also high values in the same range of permittivity for the shells with the lower level of losses. The oblate spheroidal antenna with the higher level of losses lacks of this advantage because of displacement of maximums of power and efficiency of radiation to higher magnitudes of permittivity in Fig. 2 and Fig. 3.

The normed quality factors of the antennas simulated with the approximate (19) and exact (21) formulas of the quality factor are presented in Fig. 8. Frequency derivatives of impedance components were taken for Drude's dispersion of permittivity. The spheroidal and spherical antennas in the shells with negative permittivity with low permittivity magnitude (in resonance range) have high values of the quality factor that is similar to [25]. The antennas tuned on regime of maximum power in antiresonance range (quasi-resonance) have the lowest values of the quality factor in Fig. 8. Low values of the quality factor in antiresonance range are explained by better use of the antennas volume. Because of resonance of currents, the radiating shell current goes close to the surface of the shell. Additionally, in antiresonance range both antennas are in the shells of almost spherical shape (Fig. 7).

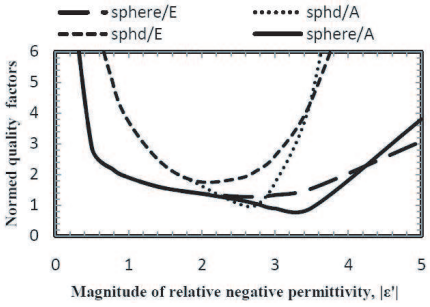


**Figure 8.** Ratio of the quality factor to the Chu limit (20) for the oblate spheroidal (sphd) and spherical (sphere) antennas in the shells as functions of magnitude of the real part of relative negative permittivity $|\varepsilon'|$ calculated with approximate (19) and exact (21) expressions and notated correspondingly by A and E.

Overall, the antennas tuned on regime of maximum power in antiresonance range provide low values of the quality factor. Optimal combination of power and efficiency of the antennas radiation and the quality factor occurs in an intermediate range of negative permittivity between resonant and antiresonant ranges of the antennas.

Exact quality factors (21) of the antennas exceed approximate quality factors calculated with (19) in antiresonant range of permittivity. Therefore, the quality factor is underestimated with the approximate formula in antiresonant range. Moreover, the approximate quality factor in Fig. 8 becomes less than the Chu limit $\left(\frac{Q}{Qlb} = 1\right)$ in antiresonance range. It is known that the quality factor approximated from antenna feed point impedance $Z_0(\omega_0)$ with (19) becomes inaccurate in the case of close resonances and antiresonance [26]. Therefore, for the first time, reliable simulation of the quality factor of the antennas in the shells with negative permittivity in antiresonance range is based on the exact formula of the quality factor (21).

## 4. CONCLUSION

Method of eigen-functions was used to calculate parameters of the oblate spheroidal and spherical antennas in the shells with negative permittivity. Calculations were done for conditions of maximal power of radiation. Calculated results have been presented as functions of negative permittivity. Calculations have shown that the antennas can be tuned on resonance by the shells with low magnitudes of negative permittivity in resonant range of the antenna. Conditions of maximum power of radiation in antiresonance range (quasi-resonance) directly continue resonance conditions in resonant range.

Similarity of quasi-resonance conditions of the antenna with condition of resonant scattering of a quasi-static electromagnetic wave by the shell with negative permittivity was found. In both cases maximal power of radiation is produced by the shell with negative permittivity. In both cases resonant polarization and dipole moment of the shell is produced by relatively small electric field of the antenna or an external source.

Optimal values of the antennas parameters correspond to different ranges of the shell permittivity. Power of radiation of the antennas tuned on resonance is higher in the middle of resonance range, while radiation efficiency is maximal in antiresonance range. The quality factors of the antennas are minimal in antiresonance range too. Wide antiresonance ranges of both antennas with the maximal

electrical size of the electrically small antennas allow optimal combining of the antenna parameters. The best combinations of the antenna parameters correspond to permittivity of the shell combining resonant and antiresonant properties of the antennas. The spherical antenna demonstrates better possible combination of the performance parameters as compared with the oblate spheroidal antenna, except for size of the shell. Optimal size of the shell with the low level of losses can be smaller for the oblate spheroidal antenna as compared with the spherical antenna.

Implementation of the discussed antennas depends on progress in technology of mediums with negative permittivity. Negative permittivity in microwave frequency range can be realized using plasma [2, 5, 6, 7], yet solid-state medium is preferable for many applications. Mediums with negative permittivity based on different kinds of LC resonators tuned on frequencies close to working frequency of the antennas is being currently intensively developed. In new designs ways to increase inductance and capacitance of LC resonators were found [27, 28]. That allows expecting of creating of a medium comprised of the LC resonators enough small size in order to be used for the shells of the electrically small antennas with negative permittivity.

## APPENDIX A. DERIVATION OF EXPRESSION FOR $W_{\mathcal{R}}(\omega_0)$

The complex far electric field pattern in spherical coordinate system [18] is

$$\mathbf{F}(\theta,\varphi) = \lim_{r\to\infty} re^{i\mathbf{k}r}\mathbf{E}(\mathbf{r}) \; . \tag{A1}$$

Link of spherical coordinate $r$ with oblate spheroidal coordinates [15] is

$$r = \frac{d}{2}\left[\left(\xi^2 - \eta^2 + 1\right)\right]^{1/2}. \tag{A2}$$

According with (7), (A1), and (A2), the complex far electric field pattern in oblate spheroidal coordinate system is

$$F(\eta,\varphi) = \lim_{\xi\to\infty}\left(\frac{\xi d}{2}\right)e^{ic\xi}E_{\eta}^{II}, \tag{A3}$$

where $E_{\eta}^{II}$ — far electric field in free space (7).

Asymptotic form of Flammer's oblate radial spheroidal function of the 4th kind for $\xi\to\infty$ [15] is

$$R_{1n}^{(4)}(-ic,\ i\xi) = \frac{1}{c\xi}\exp\left[-i\left(c\xi - \frac{n+1}{2}\pi\right)\right] + O\left(\frac{1}{\xi^2}\right). \tag{A4}$$

According with (7), (A3), and (A4) the complex far electric field pattern in oblate spheroidal coordinate system is

$$F(\eta,\varphi)=\frac{-i}{\omega\varepsilon_0}\sum_{n=1}^{\infty}g_nS_{1n}^{(1)}(-ic,\ \eta)\exp\left[i\left(\frac{n+1}{2}\pi\right)\right]. \tag{A5}$$

The energy of antenna radiation [18] in spherical coordinate system is

$$W_{\mathcal{R}}(\omega_0)=\frac{1}{2Z_f}\mathrm{Im}\int_{4\pi}F'_{I_0}F^*d\Omega, \tag{A6}$$

where $Z_f$ — impedance of free space, $\mathbf{F}=F(\theta,\varphi)$ — the complex far electric field pattern in spherical coordinates, $d\Omega=\sin\theta d\theta d\varphi$ — the solid angle integration element. According with (A5) and (A6), the energy of antenna radiation in oblate spheroidal coordinate system is

$$\begin{aligned}W_{\mathcal{R}}(\omega_0)&=\frac{1}{2Z_f}\mathrm{Im}\iint_{-1\ 0}^{1\ 2\pi}[F(\eta,\varphi)]'_{I_0}[F(\eta,\varphi)]^*d\eta d\varphi\\&=\frac{\pi}{k\omega\varepsilon_0}\mathrm{Im}\sum_{n=1,3,\ldots}^{\infty}N_{1n}(c)\,[g_n]'_{I_0}[g_n]^*,\end{aligned} \tag{A7}$$

where $[g_n]'_{I_0}$ — the frequency derivative of $g_n$ holding the feed-line current $I_0$ constant with frequency.

## REFERENCES


1. Ziolkowski, R. W. and A. Erentok, "Metamaterial-based efficient electrically small antennas," *IEEE Trans Antennas Propag.*, Vol. 54, No. 7, 2113–2130, Jul. 2006.
2. Stuart, H. R. and A. Pidwerbetsky, "Electrically small antenna elements using negative permittivity resonators," *IEEE Trans. Antennas Propag.*, Vol. 54, No. 6, 1644–1653, Jun. 2006.
3. Erentok, A. and R. W. Ziolkowski, "A hybrid optimization method to analyze metamaterial-based electrically small antennas," *IEEE Trans. Antennas Propag.*, Vol. 55, 731–741, Mar. 2007.
4. Erentok, A. and R. W. Ziolkowski, "Metamaterial-inspired efficient electrically small antennas," *IEEE Trans. Antennas Propag.*, Vol. 56, 691–7407, Mar. 2008.
5. Pistolkors, A. A. and V. I. Zimina, "Radiation of a vibrator antenna, enclosed in electron plasma," *Questions of Radio Electronics*, Vol. 12, No. 1, 3–12, 1963 (in Russian).
6. Chen, K. M. and C. C. Lin, "Enhanced radiation from a plasma-embedded antenna," *Proc. IEEE*, Vol. 56, 1595–1597, 1968.

7. Roslyakov, N. M. and N. A. Tenyakova, "Radiation of plasma-coated prolate spheroidal antenna," *Journal of Communications Technology and Electronics*, Vol. 37, No. 10, 5–14, 1992. Translated from *Radiotetechnika i Electronika*, Vol. 49, No. 4, 583–592, 1992.
8. Roslyakov, N. M., N. A. Tenyakova, and O. B. Vorob'ev (Vorobyev), "Radiation of a circular loop antenna enclosed by a magnetodielectric sphere," *Journal of Communications Technology and Electronics*, Vol. 49, No. 10, 1133–1140, 2004. Translated from *Radiotetechnika i Electronika*, Vol.49, No. 10, 1210–1217, 2004.
9. Huang, M. D. and S. Y. Tan, "Efficient electrically small prolate spheroidal antennas coated with a shell of double-negative metamaterials," *Progress In Electromagnetics Research*, PIER 82, 241–255, 2008.
10. Bichutskaya, T. I. and G. I. Makarov, "Radiation of an electric dipole from a small plasma spheroid," *Radiophysics and Quantum Electronics*, Vol. 46, No. 12, 940–947, 2003.
11. Bichutskaya, T. I. and G. I. Makarov, "Radiation from a small spheroidal antenna with plasma shell," *Radiophysics and Quantum Electronics*, Vol. 49, No. 3, 940–947, 246–257, 2006.
12. Foltz, H. D., J. S. McLean, and G. Crook, "Disk loaded monopoles with parallel strip elements," *IEEE Trans. Antennas Propag.*, Vol. 46, 1894–1896, 1998.
13. Stratton, J. A., P. M. Morse, L. J. Chu, J. D. C. Little, and F. J. Corbato, *Spheroidal Wave Functions*, John Wiley & Sons, New York,1956.
14. Flammer, C., *Spheroidal Wave Functions*, Stanford Univ. Press, California, 1957.
15. Komarov, I. V., L. I. Ponomarev, and S. Y. Slavyanov, *Spheroidal and Coulomb Spheroidal Functions*, Nauka, Moscow, 1976 (in Russian).
16. Li, L.-W., M.-S. Leong, T.-S. Yeo, P.-S. Kooi, and K. Y. Tan, "Computations of spheroidal harmonics with complex argument: A review with an algorithm," *Phys. Rev. E*, Vol. 58, No. 5, 6792–6806, Nov. 1998.
17. Falloon, P. E., P. C. Abbott, and J. B. Wang, "Theory and computation of spheroidal wave functions," *Journal of Physics A*, Vol. 36, 5477–5495, 2003.
18. Yaghjian, A. D. and S. R. Best, "Impedance, bandwidth and Q of antennas," *IEEE Trans. Antennas Propag.*, Vol. 53, No. 4, 1298–

1324, Apr. 2005.

19. Collin, R. E. and S. Rothschild, "Evaluation of antenna Q," *IEEE Trans. Antennas Propag.*, Vol. 17, No. 1, 23–27, Jan. 1964.
20. McLean, J. S., "A re-examination of the fundamental limits on the radiation Q of electrically small antennas," *IEEE Trans. Antennas Propag.*, Vol. 44, No. 5, 672–676, May 1996.
21. Best, S. R., "A Comparison of the cylindrical folded helix Q to the Gustafsson limit," *Antennas and Propagation, 2009. EuCAP 2009. 3rd European Conference in Berlin*, 2554–2557, March 23–27, 2009.
22. Stén, J. C.-E., "Radiation Q of a small antenna enclosed in an oblate spheroidal volume: Transverse-to-axis polarisation," *AEÜ. Int. Jl. Electron. Commun.*, Vol. 57, No. 3, 201–205, 2003.
23. Best, S. R., "The radiation properties of electrically small folded spherical helix antennas," *IEEE Trans. Antennas Propag.*, Vol. 52, 953–960, 2004.
24. Best, S. R., "Low Q electrically small linear and elliptical polarized spherical dipole antennas," *IEEE Trans. Antennas Propag.*, Vol. 53, 1047–1053, 2005.
25. Hirvonen, M. and S. A. Tretyakov, "Near-zero permittivity substrates for horizontal antennas: performance enhancement and limitations," *Microw. and Opt. Tech. Lett.,* Vol. 50, 2674–2677, Oct. 2008.
26. Stuart, H. R., A. D. Yaghjian, and S. R. Best, "Limitations in relating quality factor to bandwidth in a double resonance small antenna," *IEEE Antennas Wireless Propag. Lett.*, Vol. 6, No. 4, 460–463, 2007.
27. Wang, J., S. Qu, J. Zhang, H. Ma, Y. Yang, C. Gu, and X. Wu, "A tunable left-handed metamaterial based on modified broadside-coupled split-ring resonators," *Progress In Electromagnetics Research Letters*, Vol. 6, 35–45, 2009.
28. Hu, X., Q. Zhang, and S. Xe, "Compact dual-band rejection filter based on complementary meander line split ring resonator," *Progress In Electromagnetics Research Letters*, Vol. 8, 181–190, 2009.